DALTON

Crystal structure of high-spin ($S = \frac{5}{2}$) manganese(II) 2,3,7,8,12,13,17,18-octakis(ethylsulfanyl)-5,10,15,20-tetraazaporphyrinate†

Giampaolo Ricciardi,[*,a] **Alessandro Bencini,**[b] **Alfonso Bavoso,**[a] **Angela Rosa,**[a] **and Francesco Lelj**[a]

[a] *Dipartimento di Chimica, Università della Basilicata, Via N. Sauro 85, 85100 Potenza, Italy*
[b] *Dipartimento di Chimica, Università di Firenze, Via Maragliano 77, 50144 Firenze, Italy*

The crystal structure of [Mn(oetpz)] [oetpz = 2,3,7,8,12,13,17,18-octakis(ethylsulfanyl)-5,10,15,20-tetraazaporphyrinate] has been determined by single-crystal X-ray study and refined to an R value of 0.044 ($R' = 0.050$). The porphyrazine ring shows a pseudo-S_4 ruffling. The manganese atom co-ordinates within the central cavity of the macrocyclic ligand to a nearly planar array of pyrrolic nitrogen atoms, mean Mn–N$_p$ 1.927(6) Å. The intermolecular packing is reminiscent of a herringbone arrangement. Each molecule is linked to two neighbours related to it through inversion centres resulting in pseudo-octahedral metal environment with axial Mn • • • S bonds of 2.869(2) and 2.916(2) Å. Magnetic and EPR data are consistent with a weakly antiferromagnetically coupled high-spin ($S = \frac{5}{2}$) manganese(II) system. Density functional calculations indicated that such a ground spin state is unlikely for the isolated molecule. It is supposed that intermolecular interactions, mainly the axial Mn • • • S weak bonds, play a key role in determining the ground spin state experimentally found.

In a recent paper[1] we reported the synthesis of the highly soluble [M′(oetpz)] [M′ = Mn^{II}, Mn^{III}Cl or Fe^{III}Cl; oespz^{2-} = 2,3,7,8,12,13,17,18-octakis(ethylsulfanyl)-5,10,15,20-tetraazaporphyrinate (porphyrazinate)] complexes. We showed that the thioether groups attached at the periphery of the porphyrazinato ring, apart from enhancing considerably the solubility in organic solvents of these metallotetraazamacrocycles with respect to [Mn^{II}(oppz)] (oppz^{2-} = 2,3,7,8,12,13,17,18-octaphenylporphyrazinate),[2] [Mn(pc)] and [Mn(pc)Cl] (pc^{2-} = phthalocyaninate),[3] are responsible for the peculiar solid-state structure of [M(oespz)Cl] (M = Mn^{III} or Fe^{III}) complexes. They present, in fact, a stacking pattern consisting of dimers where the monomeric units are held together by long axial M^{III} • • • S interactions (see Scheme 1). Such M • • • S intermolecular interactions might play a key role in determining the liquid-crystal properties of chloroiron(III) and chloromanganese(III) octakis(octylsulfanyl)porphyrazines[4] as well as of similar alkylsulfanylporphyrazine complexes with different transition metals.[5]

It is important, therefore, to verify the occurrence of M • • • S interactions when changing the nature and/or the oxidation state of the metal. To this purpose we have undertaken a systematic study of the structural properties of a number of complexes based on oetpz. In the present paper the crystal and molecular structure of [Mn(oespz)] is reported and discussed. Since, to the best of our knowledge, this is the first structurally characterized manganese(II) porphyrazine, a special emphasis is devoted to the comparison of its molecular structure with that of porphyrin and phthalocyanine analogues. Its magnetic behaviour was investigated through variable-temperature magnetic susceptibility and EPR measurements and discussed in the light of the structural findings and molecular density functional (DF) calculations.

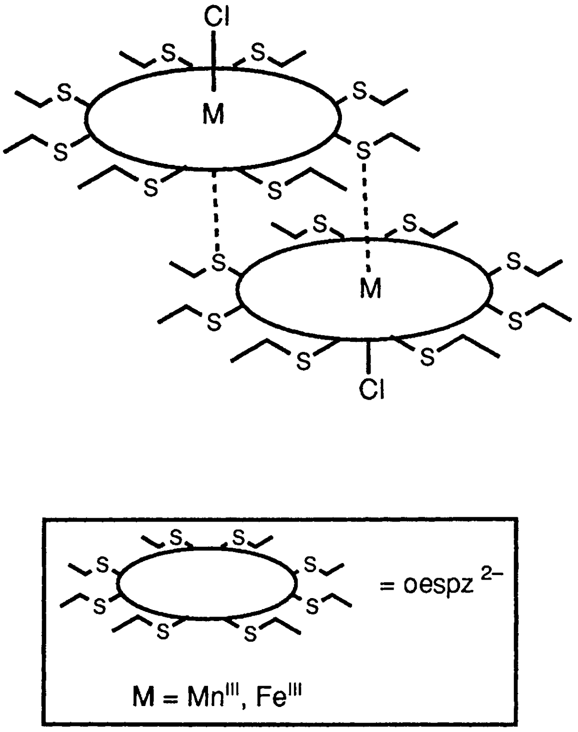

Scheme 1

Experimental

Materials

All chemicals and solvents (Aldrich Chemicals) were of reagent grade and used as supplied. Solvents used in physical measurements were of spectroscopic or HPLC grade. The compound Mn(O$_2$CMe)$_2$ was obtained from Strem. Anhydrous ethanol was obtained according to literature procedures.[6] Silica gel used for chromatography was Merck Kieselgel 60 (270–400 mesh). Air- and moisture-sensitive chemicals were handled under an inert nitrogen atmosphere using standard Schlenk techniques or in a laboratory-made glove-box.

Physical measurements

Microanalyses were performed as previously described.[1] Solution electronic spectra in 1 or 10 cm path length quartz cells in the region 200–2500 nm were recorded on a UV-VIS-NIR 05E Cary spectrophotometer, proton ^{1}H NMR spectra on an

---

† *Non-SI units employed:* $\mu_B \approx 9.27 \times 10^{-24}$ J T^{-1}, eV $\approx 1.60 \times 10^{-19}$ J.

AM 300 MHz Bruker spectrometer and polycrystalline powder EPR spectra in the temperature range 4.2–300 K using a Varian E-9 spectrometer. Liquid-helium temperature was reached with an ESR90 cryostat (Oxford Instruments). Variable-temperature magnetic measurements have been performed in the range 2.5–270 K using a Metronique Ingegnierie SQUID apparatus.

Syntheses

The compound H_2oetpz was synthesized using the procedure described for analogous alkylsulfanylporphyrazines.[1,4] The crude product was carefully purified by flash chromatography on silica gel (first band) using CH_2Cl_2–hexane (1 : 1) as eluent. (Found: C, 48.25; H, 5.25; N, 14.0; S, 32.15. $C_{32}H_{42}N_8S_8$ requires C, 48.35; H, 5.30; N, 14.1; S, 32.25%). ^1H NMR: δ_H(300 MHz, $CDCl_3$, reference $SiMe_4$) −0.95 (2 H), 1.52 (24 H, t) and 4.25 (24 H, q). UV/VIS (CH_2Cl_2): λ/nm (log ε) 360 (4.67) (Soret), 490 (4.17), 520 (4.18), 632 (4.58), 655 (4.60), 670 (sh) (4.56) and 715 (4.81) (Q bands).

The complex [Mn(oespz)] was synthesized according to the procedure previously described[1] (Found: C, 45.5; H, 4.35; N, 13.55; S, 30.15. $C_{32}H_{40}MnN_8S_8$ requires C, 45.3; H, 4.75; N, 13.2; S, 30.25%). ^1H NMR: δ_H(300 MHz, CD_3OD) 3.30 (24 H) and 4.91 (16 H).

Crystallography

Crystal data, details of data collection and structure-refinement parameters for [Mn(oespz)] are reported in Table 1, selected bond lengths and angles in Table 2. All data were collected at room temperature on an Enraf-Nonius CAD-4 diffractometer using graphite-monochromatized Mo-Kα radiation. The unit cell was determined from 25 well centred reflections. The intensity data were collected in the ω–2θ scan mode. A total of 8508 reflections were measured to θ_{max} = 27°; 3425 reflections with $I > 3\sigma(I)$ were used. Data reduction included correction for background and Lorentz-polarization effects. An absorption correction was applied according to ref. 7. The intensities of two reflections were measured every hour during data collection as a stability check of the diffractometer and the crystal; no appreciable decay in intensities was observed. The crystal orientation was checked every 200 intensity measurements using two control reflections.

Structure analysis and refinement. The structure was solved by direct methods using MULTAN.[8] The analysis of the E map derived from the set of phases with the best combined figure of merit revealed most of the non-hydrogen atoms. The remainder were located from succeeding Fourier syntheses. The structure was anisotropically refined on F by full-matrix least squares to an R value of 0.044 (R' = 0.050). The function minimized was $\Sigma w(|F_o| - |F_c|)^2$, with $w = 1$ for all the observed [$I > 3\sigma(I)$] reflections. Hydrogen atoms, included in the structural model in stereochemically calculated positions, were refined but restrained to ride on the atoms to which they are bonded. Atomic scattering factors and anomalous dispersion corrections were taken from ref. 9. All the computations were performed by the MOLEN package[10] running on a DEC VAX 6510 computer.

Atomic coordinates, thermal parameters and bond lengths and angles have been deposited at the Cambridge Crystallographic Data Centre (CCDC). See Instructions for Authors, *J. Chem. Soc., Dalton Trans.*, 1996, Issue 1. Any request to the CCDC for this material should quote the full literature citation and the reference number 186/119.

Computational details

All calculations reported were carried out with the Amsterdam density functional (ADF) program package[11,12] using the VWN parametrization[13] at the local density approximation (LDA) level and Becke's[14] and Perdew's[15] gradient corrections to the exchange and correlation energies respectively. An uncontracted double-ζ Slater atomic orbital (STO) basis was used for the ligand atoms plus polarization functions of type 3d on C, N, S and 2p on H. For Mn a triple-ζ 3d and double-ζ 3s, 3p and 4s were used, augmented with one 4p STO. The cores (C, N, 1s; Mn, S, 1s–2p) were frozen. The calculations were carried out for the [Mn(ospz)] [ospz^{2-} = 2,3,7,8,12,13,17,18-octakis(sulfanyl)-5,10,15,20-porphyrazinate] model complex using the experimental geometry (present work) of [Mn(oespz)] with appropriate averaging of bond angles and lengths to maintain a D_{4h} symmetry. The coordinate system as well as the labelling of the non-equivalent atoms in the ring used are given in Scheme 2. Multiplet energies have been computed according to the method by Ziegler *et al.*[16] The reader is directed to refs. 16–18 for worked examples of the method.

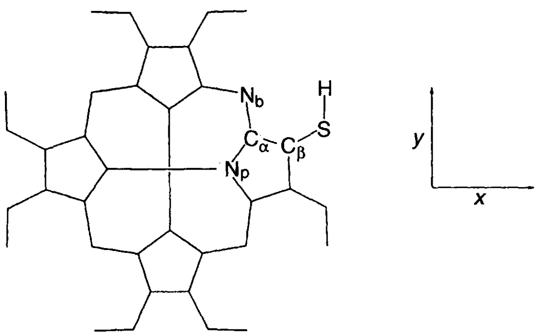

Scheme 2

Results

Characterization

Efficient purification of [Mn(oetpz)] can be achieved by repeated crystallizations of the crude product of reaction from EtOH at −90 °C under an inert atmosphere. The complex is indefinitely air stable in the solid state but strongly oxygen-sensitive in solution. Solutions of [Mn(oetpz)] in deuteriated hydrocarbons, acetonitrile, nitromethane or dimethylformamide are ^1H NMR silent. Two ^1H NMR peaks are however observed at δ 4.91 and 3.30 in CD_3OD ascribed, on integration, to the CH_2 and, respectively, CH_3 hydrogens of the ethyl groups. Fig. 1 displays the most relevant UV/VIS and near-IR absorptions of the complex. The most intense absorption in the Q-band region lies at 590 nm, a value coincident with that of the Q band of the isoelectronic [Fe(oespz)Cl][1] and blue shifted by 130 nm respect to the Q band of [Mn(pc)].[19] The energy of the Soret band is in line with the spectroscopic behaviour of mononuclear alkylsulfanylporphyrazine complexes in this region.[1,4] The complex shows two intense absorptions with an apparent vibrational structure in the 800–1500 nm near-IR region.

Molecular and crystal structure

Single crystals of [Mn(oespz)] suitable for X-ray investigation were grown in a week by freezing an ethanolic solution of the complex at −90 °C. Fig. 2 shows a view of the molecule of [Mn(oetpz)] with the numbering scheme. Atom C(20) shows high thermal paramaters probably due to disorder. Given that it involves a terminal atom of the ethyl chain, we did not attempt to solve it. The pyrroledithioether moieties of the porphyrazine ring are alternately displaced up and down leading to an apparent departure from planarity. Significant distortions of the skeleton are illustrated in Fig. 3 by the deviations from the least-squares plane of the 24-atom porphyrazinato core. The deviations tend to vanish on going from the periphery of the porphyrazine ring to the MnN_4 core which is nearly planar.

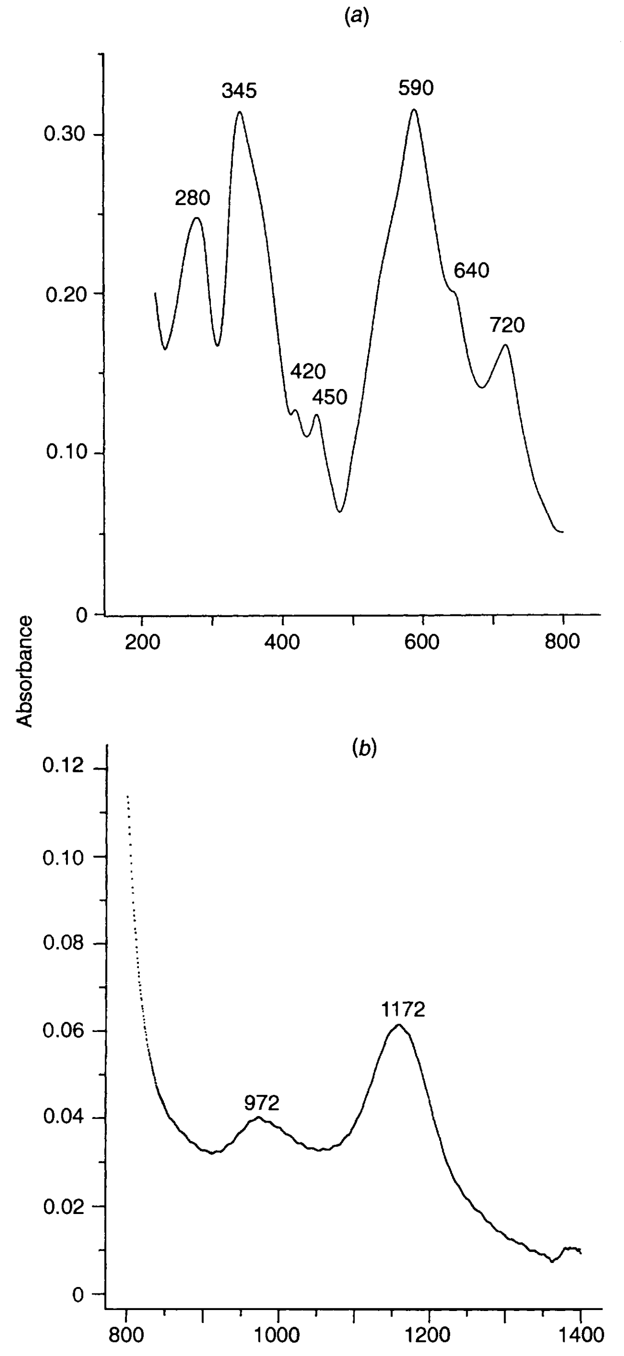

Fig. 1 Spectra of [Mn(oespz)] in EtOH under N_2: (*a*) electronic absorption, $c = 3 \times 10^{-5}$ mol dm^{-3}, in the region 300–800 nm; (*b*) NIR absorption, $c = 10^{-4}$ mol dm^{-3}, cell path length = 10 cm, scan rate = 600 nm min^{-1}

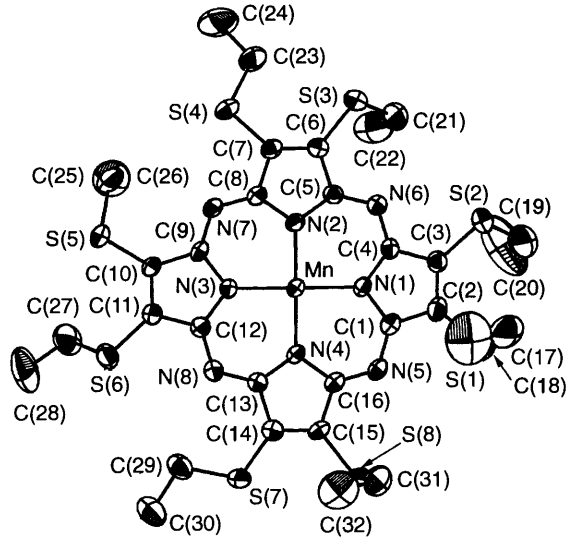

Fig. 2 An ORTEP[20] plot of [Mn(oespz)] with the atom-numbering scheme used; ellipsoids are scaled to enclose 50% electron density. Hydrogen atoms are omitted

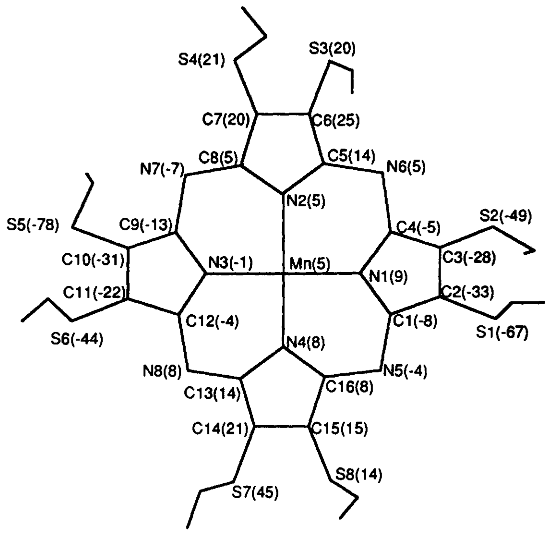

Fig. 3 Stick-bond model projection of [Mn(oespz)] along the normal to the 24-atom porphyrazinato ring illustrating the deviations of the core atoms (in 0.01 Å units) from the porphyrazinato mean plane. Estimated standard deviations are within 1 unit

Thus, while the largest displacement of peripheral sulfur atoms from the mean porphyrazine plane is 0.78(1) Å, the largest displacement of the pyrrole β-carbons is just 0.33(1) Å. The average displacement of the *meso*-nitrogens from the mean porphyrazine plane of only ≈0.05(1) Å alternating up and down is indicative of a very small saddle-like porphyrazinato core deformation. The individual pyrrole rings are essentially planar.

The dihedral angles between the four pyrrole rings and the mean porphyrazine plane are 12.1(8), 5(2), 6(2) and 4(2)°. In turn the angles between the planes of adjacent pyrrole rings span the range 17.8(6)–9(1)°. In all, the structural behaviour of the porphyrazine skeleton resembles that of a number of neutral and oxidized nickel(II) porphyrins[21] and porphyrin π-cation radicals in the solid state.[22] For instance, in the S_4-ruffled [Ni(tmp)I] (tmp = *meso*-5,10,15,20-tetramethylporphyrinate) the pyrrole rings are tilted at an angle of 12.4° with respect to the mean molecular plane, whereas the angle between adjacent pyrrole rings is approximately 17.5°.[21c]

Relevant structural parameters of [Mn(oespz)] are compared in Table 3 with those of the β-polymorph [Mn(pc)] and [Mn(tpp)] (tpp^{2-} = *meso*-5,10,15,20-tetraphenylporphyrinate).[23,24] The average C_β–C_β bond is significantly contracted with respect to the phthalocyanine complex and similar, to that of manganese(II) porphyrin.[25] The suggestion by Velàzquez *et al.*[25d] that this feature of the porphyrazinato ring should be ascribed to the electronic influence of the sulfur substituents seems to be contradicted by the fact that similar C_β–C_β bond contraction has been noticed also in ethylporphyrazine complexes. Smaller bond distances and angles associated with the nitrogen bridging group compared with the methine carbon bridge reduces the $(N_p)_4$ hole size of oetpz compared with tpp (see Table 3). As a result the inner bond distances and angles

Table 1 Data-collection and structure-refinement parameters for [Mn(oespz)]

Formula	$C_{32}H_{40}MnN_8S_8$
M_r	848.18
Crystal system	Monoclinic
Space group	$P2_1/n$
λ(Mo-Kα)/Å	0.710 73
a/Å	10.305(3)
b/Å	22.709(6)
c/Å	16.708(3)
β/°	91.4(2)
U/Å^3	3908(2)
Z	4
D_c/g cm^{-3}	1.44
μ/cm^{-1}	7.7
T/K	298
F(000)	1764
Crystal size/mm	0.3 × 0.1 × 0.05
2θ Range/°	1–27
h,k,l Ranges	−13 to 13, 0–29, 0–21
Unique reflections	8508
Observed reflections [$I > 3\sigma(I)$]	3425
Goodness of fit	2.84
No. parameters	442
Maximum Δ/σ	0.20
Maximum, minimum Δρ/e Å^{-3}	0.45, −0.12
R^a	0.044
R'^b	0.050

[a] $R = \Sigma(||F_o| - |F_c||)/\Sigma|F_o|$. [b] $R' = [\Sigma(w(||F_o| - |F_c||)^2/\Sigma w|F_o|^2]^{\frac{1}{2}}$.

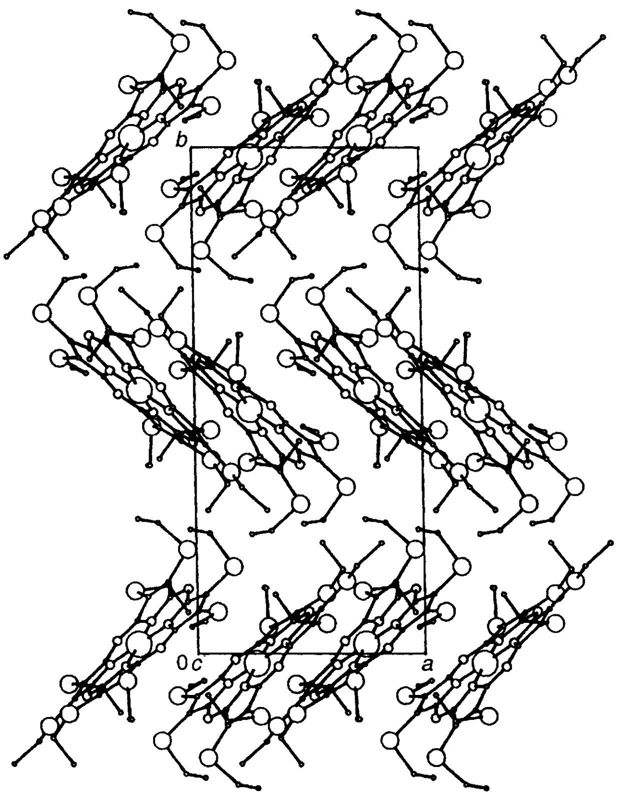

Fig. 4 A PLUTO[26] crystal-packing view of [Mn(oespz)] down the c axis. Hydrogen atoms are omitted for clarity

Table 2 Selected bond lengths (Å) and angles (°) with estimated standard deviations (e.s.d.s) in parentheses for [Mn(oespz)]. Intermolecular contacts perpendicular to the molecular plane with e.s.d.s in parentheses are also reported *

Mn–N(1)	1.931(5)	N(5)–C(16)	1.302(8)
Mn–N(2)	1.921(5)	N(6)–C(4)	1.351(8)
Mn–N(3)	1.936(5)	N(6)–C(5)	1.324(8)
Mn–N(4)	1.923(5)	N(7)–C(8)	1.312(8)
S(1)–C(2)	1.758(7)	N(7)–C(9)	1.336(8)
S(2)–C(3)	1.749(7)	N(8)–C(12)	1.335(8)
S(3)–C(6)	1.752(6)	N(8)–C(13)	1.315(8)
S(4)–C(7)	1.747(7)	C(1)–C(2)	1.430(9)
S(5)–C(10)	1.735(6)	C(2)–C(3)	1.372(9)
S(6)–C(11)	1.742(6)	C(3)–C(4)	1.431(9)
S(7)–C(14)	1.741(6)	C(5)–C(6)	1.471(9)
S(8)–C(15)	1.750(6)	C(6)–C(7)	1.342(9)
N(1)–C(1)	1.377(8)	C(7)–C(8)	1.461(9)
N(1)–C(4)	1.369(8)	C(9)–C(10)	1.449(8)
N(2)–C(5)	1.380(7)	C(10)–C(11)	1.376(8)
N(2)–C(8)	1.372(8)	C(11)–C(12)	1.432(9)
N(3)–C(9)	1.381(8)	C(13)–C(14)	1.469(9)
N(3)–C(12)	1.367(7)	C(14)–C(15)	1.344(9)
N(4)–C(13)	1.372(7)	C(15)–C(16)	1.466(9)
N(4)–C(16)	1.392(8)	C(17)–C(18)	1.49(2)
N(5)–C(1)	1.345(8)		
N(1)–Mn–N(2)	90.4(2)	N(3)–C(12)–C(11)	110.2(5)
N(1)–Mn–N(4)	178.9(2)	N(4)–C(16)–C(15)	108.3(5)
N(2)–Mn–N(3)	90.0(2)	C(1)–C(2)–C(3)	107.1(6)
N(3)–Mn–N(4)	89.4(2)	C(5)–C(6)–C(7)	106.6(5)
C(1)–N(1)–C(4)	106.7(5)	C(9)–C(10)–C(11)	106.7(5)
C(5)–N(1)–C(8)	106.6(5)	C(13)–C(14)–C(15)	107.2(5)
C(9)–N(3)–C(12)	107.1(5)	S(1)–C(2)–C(3)	129.6(5)
C(13)–N(4)–C(16)	107.4(5)	S(2)–C(3)–C(2)	132.0(5)
C(1)–N(5)–C(16)	122.2(5)	S(3)–C(6)–C(7)	129.3(5)
C(4)–N(6)–C(5)	121.4(5)	S(4)–C(7)–C(6)	136.7(5)
C(8)–N(7)–C(9)	122.0(5)	S(5)–C(10)–C(11)	123.6(5)
C(12)–N(8)–C(13)	121.7(5)	S(6)–C(11)–C(10)	131.6(5)
N(1)–C(1)–C(2)	109.5(5)	S(7)–C(14)–C(15)	124.7(5)
N(2)–C(5)–C(6)	109.5(5)	S(8)–C(15)–C(14)	127.7(5)
S(5) ··· N(1^{I})	3.222(5)	C(9) ··· C(9^{I})	3.387(8)
S(6) ··· C(5^{I})	3.430(7)	C(12) ··· C(15^{II})	3.302(8)
S(6) ··· C(6^{I})	3.452(7)	C(13) ··· C(13^{II})	3.132(8)
S(6) ··· C(7^{I})	3.528(7)	C(13) ··· C(14^{II})	3.408(9)
S(6) ··· C(8^{I})	3.547(7)		

* Symmetry codes: I $1 - x, y, 2 - z$; II $2 - x, y, 2 - z$. All intermolecular contacts are given within the limits of the van der Waals radii: N, 1.5; C, 1.75; S, 1.85 Å.

Table 3 Average bond distances (Å) and angles (°) for [Mn(pc)], [Mn(oespz)] and [Mn(tpp)]

	[Mn(pc)][a]	[Mn(oetpz)][b]	[Mn(tpp)][c]
Mn–N_p	1.933(5)	1.927(6)	2.082(2)
N_p–C_α	1.394(7)	1.376(5)	1.369(12)
C_α–C_β	1.446(8)	1.451(1)	1.445(13)
C_β–C_β	1.385(8)	1.358(5)	1.354(33)
C_α–bridging atom	1.311(9)	1.327(5)	1.412(23)
C_α–bridging atom–C_α	122.9(4)	121.8(5)	126.0(12)
C_α–N_p–C_α	106.9(5)	107.3(5)	107.6(11)
C_β–C_α–N_p	109.4(5)	108.9(5)	108.9(2)
C_β–C_β–C_α	106.9(5)	107.3(5)	107.2(12)

[a] X-Ray data from ref. 23, at 295 K. [b] For homogeneity with [Mn(pc)] and [Mn(tpp)] the parameters are symmetry averaged by imposing an idealized D_{4h} symmetry to the porphyrazine core. [c] X-Ray data from ref. 24, at 293 K.

of the oetpz ring are much closer to the corresponding ones of [Mn(pc)] and other divalent transition-metal phthalocyanines,[25b,c] than to those of [Mn(tpp)]. The C_β–S bond lengths vary from of 1.735(6) to 1.758(7) Å and the C_β–C_β–S angles range from 124.7(5) to 136.7(5)°.[25d]

The manganese atom lies in the $(N_p)_4$ plane [Δ = 0.005(1) Å] in a nearly square arrangement. The average Mn–N_p distance is 1.927(6) Å which represents, to our knowledge, the shortest such bond length for a Mn^{2+} ion co-ordinated to a tetrapyrrole donor set. The intermolecular packing (see Fig. 4) is reminiscent of a herringbone arrangement.[23] Each molecule is linked to two neighbours related to it through inversion centres at (0, 0, 0) and ($\frac{1}{2}$, 0, 0), resulting in a pseudo-octahedral metal environment with axial Mn ··· S bonds of 2.869(2) and 2.916(2) Å and

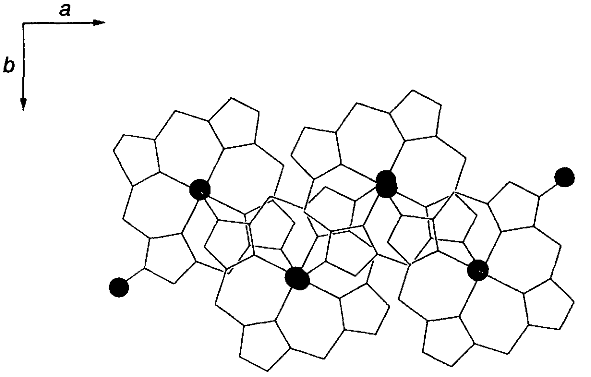

Fig. 5 Stick-bond model drawing of four molecules of [Mn(oespz)] viewed perpendicular to the 24-atom porphyrazinato mean planes showing the way in which the molecules pack to give the Mn ··· S(5), S(7) interactions. For clarity only the porphyrazinato skeleton and the sulfur atoms (shaded circles) involved in the Mn ··· S axial interaction are shown

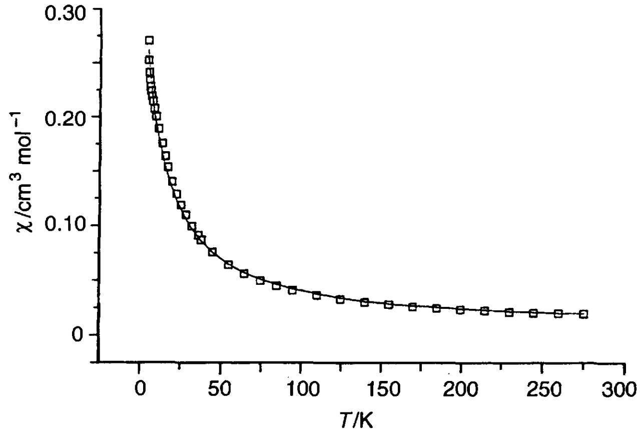

Fig. 6 Temperature dependence of the magnetic susceptibility for [Mn(oetpz)]. The solid line is the best-fit curve obtained by considering an $S = \frac{1}{2}$ paramagnetic impurity (see text)

S–Mn–S 174.4(1)°. The [Mn(oespz)] units show two modes of overlap along each molecular stack with two independent distances between the porphyrazine mean planes [3.42(2) and 3.54(2) Å] (see Fig. 5). Furthermore, the Mn ··· Mn separation is alternately 6.448(1) and 6.570(1) Å along the stack. There are a number of contacts between atoms of adjacent rings or between the outermost atoms of the porphyrazine rings and the peripheral ethyl chains. Among these interactions, only that involving the C(13) and C(13$^{\text{II}}$) atoms is unusually short, whereas a few others are within the van der Waals limit (see Table 2).[27] The remaining contacts are in the 3.5–4 Å range. Finally, there is only one significant intermolecular contact between adjacent stacks, the S(2) ··· S(3) interaction [3.72 Å, S(3) at $1 + x, y, 1 + z$], that is very close to the van der Waals limit (3.70 Å).[27]

EPR spectra and magnetic susceptibility

The polycrystalline powder EPR spectra measured in the temperature range 4.2–300 K showed an isotropic signal at $g = 2.01$ characteristic of a $S = \frac{5}{2}$ spin system with negligible zero-field splitting.

The temperature dependence of the magnetic susceptibility of [Mn(oetpz)] measured in the range 3–275 K is shown in Fig. 6. The magnetic moment at 275 K is $\mu_{\text{eff}} = 5.7\ \mu_B$, significantly higher than that expected for a $S = \frac{3}{2}$ spin system ($\mu_{\text{eff}} = 3.9\ \mu_B$) and slightly smaller than for a $S = \frac{5}{2}$ one ($\mu_{\text{eff}} = 5.9\ \mu_B$) using the spin-only formula.[28] The orbital contributions required to raise μ_{eff} from 3.9 μ_B should amount to $g = 2.95$ a value which seems too high compared to the g value previously reported for manganese(II) phthalocyanine, $g = 2.2$.[29] On the other hand a g value less than 2 is needed in order to explain the observed value of μ_{eff} if a $S = \frac{5}{2}$ spin state is assumed to be the ground state. Inspection of Fig. 6 shows no clear maximum in the χ *vs.* T curve, indicative of feeble magnetic interaction between the magnetic centres, which cannot, therefore, explain the observed value of χT at room temperature. However, a change in the curvature is observed which is indicative of the presence of some paramagnetic impurity. The magnetic data have been fitted using a Simplex minimization routine based on expression (1) which represents the magnetic susceptibility χ as

$$\chi = (1 - w)\frac{Ng^2\beta^2}{3k(T - \theta)}S(S + 1) + w\frac{Ng'^2\beta^2}{3kT}S'(S' + 1) \quad (1)$$

the sum of two contributions: the first following a Curie–Weiss behaviour,[30] the second one a Curie law. The first contribution therefore represents a weakly coupled magnetic system, the second one a paramagnetic impurity. The parameter w is the percent of paramagnetic impurity. In the fitting procedure θ, the Weiss constant, and w were considered as free parameters while $g = g' = 2$ and $S = \frac{5}{2}$ were assumed. As for the nature of such a persistent paramagnetic impurity our data seem to exclude contamination of the compound by external impurities. Repeated microanalyses on distinct sample batches were in excellent agreement with the above formulation of the complex, whereas the possible presence of extra impurities did not show up in the EPR, ^{1}H NMR or optical spectra. Theoretical results (see below) indicate that axial intermolecular interactions should play a key role in determining the observed spin state of [Mn(oespz)]. The occurrence of accidental lattice defects in the crystals, not surprising in view of the critical conditions under which the complex crystallizes, might then lead to some manganese centres with spin states different from $S = \frac{5}{2}$. Thus we have examined two hypotheses: (*i*) the presence of a manganese(II) species in the $S = \frac{3}{2}$ spin state, as usually observed in [Mn(pc)];[29] (*ii*) the presence of a manganese(II) species in the low-spin state, $S = \frac{1}{2}$. Finally, the presence of a manganese(III) impurity resulting from partial oxidation of the complex ($S' = 2$) has been also taken in consideration. Equivalent fits of the data were obtained in the three cases. A representative fitting is shown in Fig. 6 as a solid line. The best-fitting parameters are $\theta = -13.5(5)$ cm^{-1}, $w = 4.3(8)\%$ for $S' = 2$ and $\theta = -13.2(7)$ cm^{-1}, $w = 1.2(3)\%$ for cases (*i*) and (*ii*) respectively. The measured θ value is independent of the nature of the impurity, while, of course, changing the spin of the impurity from 2 to $\frac{3}{2}$ to $\frac{1}{2}$ reduces the percentage of impurity required to reproduce the data.

In agreement also with the EPR findings, the observed magnetism of [Mn(oespz)] is therefore ascribed to a weakly antiferromagnetically coupled high-spin manganese(II) system containing a small percent of paramagnetic impurity.

Discussion

Structure

The molecular structure of [Mn(oespz)] reveals that the oetpz central cavity is considerably contracted with respect to that of tpp and slightly smaller than that of pc.[28] This, together with the fact that the Mn atom is placed in the $(N_p)_4$ plane of the oetpz ligand, imposes a Mn–N$_p$ distance much shorter than that observed in [Mn(tpp)] and slightly shorter than that in [Mn(pc)]. This short distance is indicative of strong $N_p \rightarrow Mn$ σ donation and Mn$\rightarrow$(oespz) π^* back donation.[25,31]

As for the Mn ··· S interactions, they are induced by the axially unsaturated manganese(II) centre. By itself, in fact, the thioether function is a weak ligand for metal ions because of its poor σ-donor and π-acceptor character.[32] Ligands with special stabilizing features like multidenticity or anionic charge[33,34] or highly unsaturated metal centres constrained in a tetrapyrrole donor set are required for viable thioether co-ordination.[35]

Among the few $Mn^{II}\cdots S$ (thioether) bonds structurally characterized at present those in [Mn(oespz)] are the longest; $Mn^{II}\cdots S$ bonds spanning the range 2.677(3)–2.783(4) Å have recently been found in a family of high-spin complexes which incorporate an $Mn^{II}\cdots S$ (thioether) bond in a distorted-octahedral $MnS_2N_2O_2$ co-ordination sphere.[34] Much shorter Mn–S bond lengths [2.350(5) Å] have been found in an unusually low-spin complex of co-ordination type MnS_2N_4.[33] The $Mn^{II}\cdots S$ interactions are quite shorter than the $Mn^{III}\cdots S$ axial interactions occurring in the parent complex [Mn^{III}(oespz)Cl] [$Mn^{III}\cdots S$ 3.231(1) Å].[1] This seems to be at variance with recent structural findings according to which the average $Mn\cdots S$(thioether) bond length decreases by ≈0.2 Å in the trivalent metal species, consistent with radial contraction of manganese upon oxidation.[33,34] However, our data can be, partly reconciled with the literature by considering that: (*a*) the manganese(III) centre is, in the [{Mn^{III}(oetpz)Cl}$_2$] structure (Scheme 1), extruded out of the $(N_p)_4$ donor set in the direction of the apical chlorine, the distance between the metal atom and the centre of the basal plane being 0.291(1) Å; (*b*) the inter-ring repulsions probably, prevent, a stronger $Mn^{III}\cdots S$ interaction.[1]

The porphyrazine core deviates from planarity to minimize interring and ethylsulfanyl–ring steric repulsions. In line with the 'hybrid' structure of the porphyrazines, the distortions of the porphyrazinato ring are larger than those observed in the porphyrazinato core of [M(pc)] (M = Mn, Mg, Co, Ni or Co),[23,25a] but smaller than those usually found in S_4-ruffled metalloporphyrins.[21,22]

High-spin character

Magnetic susceptibility and EPR data unambiguously point to a high-spin ($S = \frac{5}{2}$) ground state for [Mn(oespz)]. Such a ground state has also been found for [Mn(tpp)][24] and ascribed to the large central cavity of the tpp ligand and to the out-of-plane displacement of the manganese atom. It has been suggested that these structural features, weakening the interaction between the manganese $d_{x^2-y^2}$ orbital and the nitrogen lone pairs, stabilize the $Mn–N_p$ strongly σ-antibonding $d_{x^2-y^2}$ orbital which becomes suitable for partial occupation (see, for instance, also ref. 3, p. 526). The smaller central hole size of the pc ring compared to that of tpp and the placement of the Mn atom in the plane of the pyrrole nitrogen donors have been considered, in turn, responsible for the unusual intermediate spin ($S = \frac{3}{2}$) ground state of [Mn(pc)].[32,36] In this case the σ-antibonding $d_{x^2-y^2}$ orbital would be, in fact, too high lying to be occupied, a suggestion confirmed by HFS DV-Xα calculations by Reynolds and Figgis[37] which predict for [Mn(pc)] a ^4E_g ground state that is, for the free ion, the $(d_{xy})^1(d_\pi)^3(d_{z^2})^1(d_{x^2-y^2})^0$ configuration.

Based on the above arguments one would expect the [Mn(oespz)] complex, where the $Mn–N_p$ distance is very similar to that found in [Mn(pc)], to have an intermediate spin rather than the high-spin ground state experimentally found. That electronic structure effects of the peripheral sulfur atoms may lead to a $S = \frac{5}{2}$ spin state for [Mn(oespz)] cannot be, however, *a priori* excluded. Furthermore, unlike in [Mn(tpp)] and [Mn(pc)], the mangenese centre in [Mn(oespz)] is weakly bonded to the peripheral sulfur atoms of adjacent molecules. In order to answer the question whether the $S = \frac{5}{2}$ ground spin state found for [Mn(oetpz)] is an intrinsic characteristic of the isolated molecule or rather a consequence of axial interactions, we have performed DF calculations on the [Mn(ospz)] model system. In particular we addressed the question whether this system would prefer a $S = \frac{5}{2}$ spin state or, just like [Mn(pc)], a $S = \frac{3}{2}$ state.

It is well known that in the case of symmetrical molecules with degenerate orbitals, as it is for [Mn(ospz)] in D_{4h} symmetry, the individual multiplet states arising from an open-shell configuration cannot, in general, be expressed by a single determinant. That is, DF calculations do not yield multiplet energies directly. According to the method of Ziegler *et al.*[16] it is possible to express the energy of multiplets arising from a given configuration as a weighted sum of single-determinant energies. In the case at hand, there is only one configuration with five unpaired electrons, $[e_g(d_\pi)]^2[b_{1g}(d_{xy})]^1[a_{1g}(d_{z^2})]^1[b_{2g}(d_{x^2-y^2})]^1$ compatible with a d^5-manganese(II) system. It gives rise to the $^6A_{1g}$ state. There are on the contrary a number of possible one-electron configurations with three unpaired electrons. These give rise to many quartet states. The determination of their relative energies is a lengthy calculation[16,38] within the DF framework since, as stressed above, it implies the calculations of many single-determinant energies. Furthermore, certain multideterminant states can be resolved only by evaluating some two-electron integrals.[17] This is outside the scope of the present paper. Thus, we restricted ourselves to the determination of the energy of one quartet state, the ^4E_g derived from the free-ion $(d_{xy})^1(d_\pi)^3(d_{z^2})^1(d_{x^2-y^2})^0$ configuration. This state is of interest, since it has been proved to be the ground state for manganese(II) phthalocyaninate. From our calculations the $^6A_{1g}$ state is 1.94 eV (15650 cm^{-1}) less stable than the ^4E_g. Although these calculations do not allow us to state that ^4E_g is the ground state of the molecule (knowledge of the energies of all quartet and doublet states would be needed),* nevertheless they clearly exclude a $S = \frac{5}{2}$ ground state for the [Mn(ospz)] model system.

The computed $^6A_{1g}/^4E_g$ energy splitting for the model system is expected to remain the same when the molecule assumes the distorted experimental geometry. Actually, calculations on $ospz^{2-}$ indicate that the one-electron levels change very little in energy (less than 0.05 eV) and composition on going from D_{4h} to the C_1 experimental structure. Furthermore, it has been demonstrated that S_4 ruffling of the porphyrin ring induces only negligible effects on the electronic structure of iron(III) porphyrins.[32d] Similarly, saddle-like distortion of the ligand was found to modify only slightly the orbital pattern of copper(II) tetraazaannulene.[39]

Therefore the observed $S = \frac{5}{2}$ ground spin state for [Mn(oespz)] is most likely related to the modifications of the orbital pattern of the isolated molecule induced by the axial $Mn\cdots S$ interactions between adjacent molecules, consisting essentially in a splitting of the [Mn(oespz)] frontier orbitals having large d_π and d_{z^2} character. Although a quantitative estimate of these splittings is prevented by the size of the system, it is reasonable to suppose that they are quite small due to the large $Mn\cdots S$ distance. Thus, the presence of closely spaced levels susceptible to partial occupation, together with the large spin-pairing energy of the manganese(II) ion,[40] would favour a high-spin system. Notably this high-spin situation will never involve the high-lying $d_{x^2-y^2}$ metal orbital, in agreement with the very short Mn–N distance experimentally observed.

Conclusion

We have presented the first investigation of the structural and magnetic properties of a manganese(II) porphyrazine. The molecular structure of [Mn(oespz)] shows a pseudo S_4 ruffling of the porphyrazine core, a common feature for porphyrin

---

* It is worth noting however that among the single-determinant doublet states derived from a free-ion configuration with only one unpaired d-electron, the lowest one, the ^2E_g, is 2.0 eV less stable than the ^4E_g state.

macrocycles but never observed in porphyrazinic rings. The complex exhibits a Mn–N_p distance slightly shorter than that of [Mn(pc)] and, hence, the shortest one among those found in manganese(II) tetrapyrroles. The herringbone-like arrangement of the intermolecular packing results in a pseudo-octahedral metal environment with long axial Mn $\cdots$ S bonds. Magnetic and EPR data are consistent with a weakly antiferromagnetically coupled high-spin ($S = \frac{5}{2}$) manganese(II) system. Density functional calculations indicated that a $S = \frac{5}{2}$ ground spin state is quite unlikely for the isolated molecule. It is supposed that intermolecular interactions, mainly the weak axial Mn $\cdots$ S bonds, play a key role in the experimentally determined $S = \frac{5}{2}$ ground spin state.

Acknowledgements

Thanks are expressed to Dr. A. Caneschi, University of Firenze, for performing magnetic measurements, to Mr. S. Laurita for collecting X-ray data and to Mr. C. Barlabà for technical support. Financial support from Ministero della Università e della Ricerca Scientifica e Tecnologica (MURST) and from Consiglio Nazionale delle Ricerche (CNR) is also gratefully acknowledged.

References

1 G. Ricciardi, A. Bavoso, A. Bencini, A. Rosa, F. Lelj and F. Bonosi, *J. Chem. Soc., Dalton Trans.*, 1996, 2799.

2 M. J. Camenzind and C. L. Hill, *Inorg. Chim. Acta*, 1985, **99**, 63.

3 L. J. Boucher, in *Coordination Chemistry of Macrocyclic Compounds*, ed. G. A. Melson, Plenum, New York, 1979, p. 527 and refs. therein.

4 G. Ricciardi, F. Lelj and S. Belviso, unpublished work.

5 F. Bonosi, G. Ricciardi, F. Lelj and G. Martini, *J. Phys. Chem.*, 1993, **97**, 9181; 1994, **98**, 10613; G. Ricciardi, F. Lelj and F. Bonosi, *Chem. Phys. Lett.*, 1993, **215**, 541; F. Lelj, G. Morelli, G. Ricciardi, A. Roviello and A. Sirigu, *Liq. Cryst.*, 1992, **12**, 6, 941.

6 D. D. Perrin and W. L. F. Armarego, *Purification of Laboratory Chemicals*, 3rd edn., Pergamon, Oxford, 1988.

7 N. Walker and D. Stuart, *Acta Crystallogr., Sect. A*, 1983, **39**, 159.

8 G. Germain, P. Main and M. M. Woolfson, *Acta Crystallogr., Sect. A*, 1971, **27**, 368.

9 *International Tables for X-Ray Crystallography*, Kynoch Press, Birmingham, 1974, vol. IV, p. 99.

10 C. K. Fair, MOLEN, Structure Determination System, Delft, 1990.

11 E. J. Baerends, D. E. Ellis and P. Ros, *Chem. Phys.*, 1973, **2**, 42; E. J. Baerends and P. Ros, *Int. J. Quantum Chem.*, 1978, **S12**, 169.

12 P. M. Boerrigter, G. te Velde and E. J. Baerends, *Int. J. Quantum Chem.*, 1988, **33**, 87; G. te Velde and E. J. Baerends, *J. Comput. Phys.*, 1992, **99**, 84.

13 S. H. Vosko, L. Wilk and M. Nusair, *Can. J. Phys.*, 1980, **58**, 1200.

14 A. D. Becke, *J. Chem. Phys.*, 1986, **84**, 4524; *Phys. Rev. A*, 1988, **38**, 3098.

15 J. P. Perdew, *Phys. Rev. B*, 1986, **33**, 8822; **34**, 7406.

16 T. Ziegler, A. Rauk and E. J. Baerends, *Theor. Chim. Acta*, 1977, **43**, 261.

17 R. M. Dickson and T. Ziegler, *Int. J. Quantum Chem.*, 1995, 1996, **58**, 681.

18 C. Daul, E. J. Baerends and P. Vernooijs, *Inorg. Chem.*, 1994, **33**, 584.

19 A. B. P. Lever, P. C. Minor and J. P. Wilshire, *Inorg. Chem.*, 1981, **20**, 2550.

20 C. K. Johnson, ORTEP, Report ORNL-5138, Oak Ridge National Laboratory, Oak Ridge, TN, 1976.

21 (*a*) A. Ulmann, J. Gallucci, D. Fisher and J. Ibers, *J. Am. Chem. Soc.*, 1980, **102**, 6852; (*b*) J. C. Gallucci, P. N. Swepston and J. Ibers, *Acta Crystallogr., Sect. B*, 1982, **38**, 2134; (*c*) E. F. Meyer, Jr., *Acta Crystallogr., Sect. B*, 1972, **28**, 2162; (*d*) L. J. Pace, J. Martinsen, A. Ulmann, B. M. Hoffman and J. A. Ibers, *J. Am. Chem. Soc.*, 1983, **105**, 2612.

22 (*a*) P. Gans, G. Buisson, E. Duee, J.-C. Marchon, B. S. Erler, W. F. Scholz and C. A. Reed, *J. Am. Chem. Soc.*, 1986, **108**, 1223; (*b*) W. R. Scheidt and Y. J. Lee, *Struct. Bonding (Berlin)*, 1987, **64**, 1.

23 J. F. Kirner, C. A. Reed and W. R. Scheidt, *J. Am. Chem. Soc.*, 1977, **99**, 1093.

24 R. Mason and G. A. Williams, *J. Chem. Soc., Dalton Trans.*, 1979, 677.

25 (*a*) J. Fitzgerald, B. S. Haggerty, A. N. Rheingold and L. May, *Inorg. Chem.*, 1992, **31**, 2006; (*b*) N. Yaping, J. Fitzgerald, P. Carroll and B. B. Wayland, *Inorg. Chem.*, 1994, **33**, 2029; (*c*) A. Ghosh, J. Fitzgerald, P. G. Gassman and J. Almlof, *Inorg. Chem.*, 1994, **33**, 6057; (*d*) C. S. Velázquez, G. A. Fox, W. E. Broderick, K. A. Andersen, O. P. Anderson, A. G. M. Barrett and B. M. Hoffman, *J. Am. Chem. Soc.*, 1992, **114**, 7416.

26 W. O. S. Motherwell and W. Clegg, PLUTO 78, Program for plotting molecular and crystal structures, University of Cambridge, 1978.

27 L. Pauling, *The Nature of the Chemical Bond*, 3rd edn., Cornell University Press, Ithaca, NY, 1960.

28 O. Khan, *Molecular Magnetism*, VCH, New York, 1993.

29 C. G. Barraclough, R. L. Martin, S. Mitra and R. C. Sherwood, *J. Chem. Phys.*, 1970, **53**, 1638.

30 A. S. Chakravarty, *Introduction to the Magnetic Properties of Solids*, Wiley, New York, 1980.

31 A. Takenaka, S. K. Syal, Y. Sasada, T. Omura, H. Ogoshi and Z. Yoshida, *Acta Crystallogr., Sect. B*, 1976, **32**, 62.

32 (*a*) S. E. Livingston, *Q. Rev. Chem. Soc.*, 1965, **19**, 386; (*b*) S. G. Murray and F. R. Hartley, *Chem. Rev.*, 1981, **1**, 365; (*c*) S. R. Cooper and S. C. Rawle, *Struct. Bonding (Berlin)*, 1990, **72**, 1; (*d*) D. H. Jones, A. Scott Hynman and T. Ziegler, *Inorg. Chem.*, 1993, **32**, 2092.

33 S. Karmakar, S. B. Choudhury and A. Chakravorty, *Inorg. Chem.*, 1994, **33**, 6148.

34 P. Chakraborty, S. K. Chandra and A. Chakravorty, *Inorg. Chem.*, 1993, **32**, 5349.

35 T. Mashiko, C. A. Reed, K. J. Haller, M. E. Kastner and W. R. Scheidt, *J. Am. Chem. Soc.*, 1981, **103**, 5758; J. McKnight, M. R. Cheesman, C. A. Reed, R. D. Orosz and A. J. Thomson, *J. Chem. Soc., Dalton Trans.*, 1991, 1887; S. Karmakar, S. B. Choudhury and A. Chakravorty, *Inorg. Chem.*, 1994, **33**, 6148; M. Tomita, N. Matsumoto, H. Akagi, H. Okawa and S. Kida, *J. Chem. Soc., Dalton Trans.*, 1989, 179.

36 C. G. Barraclough, A. K. Gregson and S. Mitra, *J. Chem. Phys.*, 1974, **60**, 962; H. Miyoshi, *J. Phys. Soc. Jpn.*, 1974, **37**, 50; H. Miyoshi, H. Ohya-Nishiguchi and Y. Deguchi, *Bull. Chem. Soc. Jpn.*, 1973, **46**, 2724.

37 P. A. Reinolds and B. N. Figgis, *Inorg. Chem.*, 1991, **30**, 2294.

38 C. Daul, *Int. J. Quantum Chem.*, 1994, **52**, 867.

39 G. Ricciardi, A. Bavoso, A. Rosa, F. Lelj and Y. Cizov, *J. Chem. Soc., Dalton Trans.*, 1995, 2385.

40 A. B. Lever, in *Inorganic Electronic Spectroscopy*, 2nd edn., Elsevier, New York, 1984, p. 750.

Received 7th March 1996; *Paper* 6/01627H